Seismic Behaviour of Spent Fuel Racks in Different Configurations of Support Design

D. Bouche-Pillon, F. Le Breton, A. Thouvenot
Framatome, Tour Fiat Cedex 16, F-92084 Paris la Défense, France

SUMMARY

The seismic behaviour of spent fuel storage racks is a major concern for safety purposes. Racks are submerged in water in the spent fuel pool of a nuclear power plant and consist of an array of individual cells which are usually interconnected with top and bottom grid structures to form integral modules. Owing to the possible tilting of fuel assemblies in the cells, in an earthquake event, specific supporting devices must be designed, for seismic purpose, in order to reduce induced loads in structures, e.g. fuel assemblies, racks and pool walls. The paper presents a generic study on the seismic behaviour of fuel racks in different configurations of support design :

- rigidly supported
- free-standing (sliding and rocking)
- aseismic device.

The seismic excitation is transmitted to each fuel assembly by the supporting structures. The use of time history accelerations developed from floor response spectra is discussed. The finite element model used for the nonlinear dynamic analysis of the whole structure must be optimized for cost and accuracy purposes. It must be representative of nonlinearities between fuel assemblies and cells (clearances and friction). It must also take into account the hydrodynamic effects coupling fuel assemblies, cells and pool walls. The size of the model depends on the behaviour of supports. Generally bidimensionnal analyses are adequate to study the general stability of the structures.

The assumptions made in the model on the following items :

- structural damping of cells and fuel assembly
- impact stiffness and damping of grid assembly
- hydrodynamic effects
- friction laws
- specific behaviour of supports

must be qualified by means of experimental studies.

The paper documents the repartition of loads on the racks, on the pool walls and on the fuel assembly. Fluid coupling effects are presented.

1. INTRODUCTION

The storage of spent fuel assemblies in the fuel building pools of the French 1300 MW PWR is realized in 5 m height racks immersed under 8 m water.

Several designs of connection between racks and pool exist. They must allow thermal expansion and insure safety in an earthquake event. Fuel assemblies are stored in the cells of the racks and can move inside with a significant gap (about 1 cm for overall dimensions 20 cm x 20 cm).

During seismic event, the combined vibratory movement of pool, racks, fuel assemblies, water, couples mechanical and hydrodynamic phenomena induced by tilting in water medium of fuel assemblies in cells, vibrations of cells in water, movements of pool, water flow, hydrostatic buoyancy, shocks, etc...

It is necessary to define separately each phenomenon and to study the whole behaviour in order to calculate loads on the pool walls and floor, on the racks and on the fuel assemblies.

This study presents results of a nonlinear transient analysis of fuel racks models in different support configurations.

- Design 1 : rigidly supported racks at top and bottom
- Design 2 : freestanding racks
- Design 3 : racks on aseismic bearing devices (DAP)

2. FINITE ELEMENT MODEL OF FUEL RACK SYSTEM

2.1. Law of similars

Numerical studies show the quick phasing of fuel assemblies having different initial positions in cells. Consequently the analysis of one fuel assembly in one cell simulates the response of full fuel assembly rack module loadings. The law of similars maintains displacements, accelerations, velocities, stresses but reduces masses and loads proportionally to the number of cells.

2.2. Mechanical model (figure 1)

Cell and fuel assembly are modelled with 2-D beam elements including shear effects. The number of nodes in the model is representative of the grid assembly number.

Links between fuel assembly and cell simulate the eventual contact forces between grids and cell. Nonlinear dynamic elements including a gap J, a spring K and a viscous damper C connect adjacent nodes of fuel and cell.

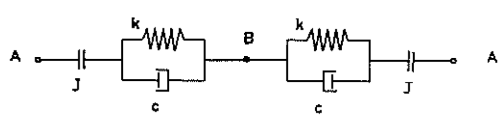

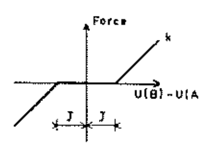

The initial value of J is determined while assuming that fuel assembly is centered in cell. K and C are experimental values.

Coulomb friction at the bottom of fuel assembly is modelled with a nonlinear element restituting a bilinear law of friction and sliding. The maximum sliding force is related to the normal load by the steel-steel friction coefficient. For numerical reasons, a small displacement D_s of the fuel assembly bottom is permitted by a local stiffness before sliding occurs.

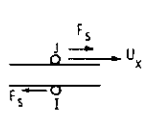

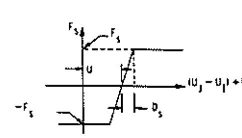

The percentage of critical damping value ξ is 12 % for the fuel assembly (experimental data) and 3 % for the cell. The damping matrix $|C|$ is the linear function of the mass $|M|$ and stiffness $|K|$ matrices, defined by :

$$|C| = 4\pi \frac{fr \cdot fs}{fr + fs} \xi \, |M| + \frac{\xi}{\pi \, (fr + fs)} \, |K| \qquad (1)$$

where fr = 2 Hz and fs = 20 Hz for the fuel assembly
fr = 6 Hz and fs = 30 Hz for the cell

Motions are investigated in only one vertical plane. Thus, the out of plane degree of freedom are fixed.

2.3. Fluid - structure interaction

2.3.2. Theory

The fundamental equation for dynamic problems without fluid coupling is :

$$|Ms|\ \{\ddot{u}\} + |C|\ \{\dot{u}\} + |K|\ \{u\} = -|Ms|\ \{\gamma\} + |Fps| \qquad (2)$$

where $|K|, |C|, |Ms|$ stiffness, damping and solid mass matrices
$\{u\}, \{\dot{u}\}, \{\ddot{u}\}$ displacement, velocity and acceleration vector relative to base motion.
$\{\gamma\}$ pool absolute acceleration
$|Fps|$ pseudoforces vector accounting for nonlinearities.

The fluid motion is considered to be described by incompressible potential flow, so that the dynamic fluid effect on the fuel rack system can be accounted for by hydrodynamic mass. According to Fritz in reference (1) and neglecting the viscosity effect, fluid-structure interaction between the racks and the pool lead to :

$$(|Ms| + |Mh|)\ \{\ddot{u}\} + |C|\ \{\dot{u}\} + |K|\ \{u\} = -\ (|Ms| - |Md|)\ \{\gamma\} + |Fps| \qquad (3)$$

where $|Mh|$ added mass matrix
$|Md|$ mass matrix of fluid displaced by the solid.

Comparison between eq. (2) and (3) shows that :

- The apparent mass of the structure increases
- The inertial force induced on the structure by the acceleration γ is reduced by $|Md|\ \{\gamma\}$.

2.3.2. Modelling fluid coupling effects

Fluid interaction between cell and fuel assembly is modelled by non diagonal mass matrices coupling each level (see figure 1) :

$$|MA| = \begin{vmatrix} +\ m_{h1} & -\ (m_{h1} + m_{d1}) \\ -\ (m_{h1} + m_{d1}) & +\ (m_{h1} + m_{d1} + m_{e1}) \end{vmatrix} \qquad (4)$$

where m_{h1} : added mass on fuel assembly
m_{d1} : mass of fluid displaced by fuel assembly
m_{e1} : mass of fluid entrapped in cell without fuel assembly.

Fluid interaction between cell and pool is obtained by loading each node of cell with :

m_{h2} : added mass
$F = (m_{h2} + m_{d2})\ \gamma$: external fluid force (5)
where m_{d2} : mass of fluid displaced by the cell.

The hydrodynamic load induced on the pool is calculated by :

$$Fp = (m_{h2} + m_{d2})\ \{\ddot{u}\} - m_{e2}\ \{\gamma\} \qquad (6)$$

where m_{e2} : mass of fluid entrapped in the pool in the absence of racks.

Added and displaced fluid masses are determined by experimental and numerical methods, as a function of the racks arrangement. For these masses there is no added damping.

2.4. Seismic excitation : (figures 3 and 4)

Considering the planar model and for sake of simplicity, only the seismic excitation in the horizontal direction is applied. The accelerogram is synthesized by the computer code TIROIR reference (2) from the SSE floor response spectrum at pool floor level.The probabilist method used, generates randomly phase angles for the sine waves.

2.5. Numerical methods

The nonlinear dynamic equations given in § 2.3.1. are solved by direct integration, using the Newmark Beta integration scheme, with a time step Δt = 0,002 sec.. At any time t, the relative acceleration $\ddot{u}$ of a node is computed from its relative displacement u by :

$$\ddot{u}\ (t) = \{u(t - \Delta t)\ - 2\ u\ (t) + u\ (t + \Delta t)\}\ /\ (\Delta t)^2 \qquad (7)$$

2.6. Support design

The fuel rack system models shown in figures 2 through 4 are one-cell representations of a fully loaded rack.

2.6.1. Design 1 : Top and bottom fixed racks (Figure 2)

A rigid linear spring is modelled at each end of the cell in the horizontal direction. At the top end, the spring represents the immersed hydraulic jaks which allow the racks thermal expansion but restrain seismic displacement. At the bottom end, the spring represents the anchors in the pool floor.

2.6.2. Design 2 : Freestanding racks (Figure 3)

The beam elements which model the baseplate and support pads, have stiffness properties which are rigid relative to the seismic excitation, and have a 3 % damping value (fr = 6 Hz, fs = 30 Hz). A nonlinear friction element, similar to the one used for the fuel assembly, models the sliding of the support pads on the pool floor. Nonlinear dynamic elements with one gap connected to one spring, models the vertical links between the support pads and the pool floor.

2.6.3. Design 3 : Racks on aseismic bearing devices (DAP) (Figure 4)

The DAP are supporting devices on which the racks are resting. They comprises two superposed pair of horizontal roller bearings between three independant supporting parts. They are modelled by an adequate finite element which compute at any time the reaction force between the pool floor and the cell, with respect to its technological and physical characteristics.

3. RESULTS (For one storage cell)

The maximal values of results are summarized in table 1 for the three configurations of support. Figures 7 through 18 show curves versus time of typical responses. It is clearly established that each response is the sum of a stationary response and a shock response with high amplitudes and short duration.

Reaction forces (Figures 7 through 9)

The maximal horizontal reaction forces are obtained in design 1 (Figures 7 and 8). Maximal values at top on the jaks and at bottom on the anchors, are respectively equal to 1.8 and 1.3 times the loaded cell weight (10.1 kN). In design 2, the horizontal reaction force at bottom is limited by sliding. In desigh 3, this horizontal reaction force is nearly zero. The vertical reaction forces are no much modified by the horizontal seismic excitation in design 1 and 3.But in design 2, the rack lift-off creates vertical impact forces, whose values are about 4 times the loaded cell weight (Figure 9).

Hydrodynamic pool loads (Figures 10 through 12)

The maximum value of the hydrodynamic horizontal pool reaction force Fp (eq. 5) is equal to 1,6 times the loaded cell weight in design 1 and 2, while it is 20 % reduced in design 3. The hydrodynamic force Fp is the sum of the hydrodynamic force Fr created by racks and of the hydrodynamic force Fe induced by the pool water. The maximum Fe value, 3.5 kN for 5 m pool height, exists in the abscence of racks. The Fr force shows the fluid coupling effect between pool and racks. Its maximum value is equal to 4 times Fe value in design 1. Figures 10 through 12 show that the Fp high frequency content is poor in design 3.

Hydrodynamic cell loads (Figures 13 through 15)

The maximum hydrodynamic cell force Fa is obtained in design 2 and is equal to 2.1 times the loaded cell weight. In design 3 this value is 24 % reduced.

Fuel assembly - cell impact loads (Figures 16 through 18)

The impact force Fc of a nonlinear link element connecting fuel assembly and cell, is the sum of spring and viscous damper forces. These two forces are not in phase and the spring force is the biggest. Fc maximum value, obtained in design 1 and 2, is equal to 1.5 times the fuel assembly weight (8.2 kN), while in design 3, it is 28 % reduced. The impact duration is 0,03 sec. The maximum value of the sum Fct of all impact forces on fuel assembly is about twice Fc value. At fuel assembly bottom there is no impact, due to friction. Fct plots show that impacts are not simultaneous on all grids.

Cell relative displacement

In design 2, the support pad lift-off induces a general rotational motion with a maximum horizontal displacement of 63 mm at the cell upper end. In design 3, the maximum amplitude of the roughly translational motion is 28 mm. In design 1, the maximum displacement value is only 3 mm.

Interpretation

Several support designs have been analysed. It is clearly shown that softening the connection between racks and pool, considerably reduces loads on structures. Free racks translation (design 3) is better than free rotation (design 2)because no vertical impact load is induced by horizontal accelerations and horizontal loads on pool walls, fuel assemblies and racks are appreciably reduced. The validity of that theoretical principle is justified by tests.

4. DESCRIPTION AND QUALIFICATION

Each aseismic bearing device comprises two superposed pairs of horizontal roller bearings, the axes of one pair being perpendicular to the axes of the other pair, and three independent supporting parts. A guiding device enhances the working reliability. The whole system has been patented by Framatome.

Two series of tests have been performed to qualify the principle and its technological realisation.

The firt serie of in air tests of a 1/4 scale rack model, put on a triaxial shaker table (three independant motions), shows the dynamic characteristics of the DAP and their capacity to transmit only attenuate horizontal vibrations, for several loading cases. The finite element used in § 2.6.3 is also qualified by this experimentation.

The second serie of tests analyses the behaviour of an 1/10 scale pool model comprising compact storage racks on DAP. Results confirm the possibility to apply the Fritz theory to this kind of structure and indicate that Mh is about 2.5 Md. The pool sloshing has no major effect on the whole behaviour, but disymetrical rack loading induces a yawing motion, superposition of a rotational motion to a translational one. Nevertheless this secondary phenomenon generates small additional translations in the direction perpendicular to the excitation one. Finally viscous fluid effects, which tend to restrain relative displacements, are important (ξ = 15 %) in the 1/10 scale model, but do not affect the good working of DAP.

5. CONCLUSION

The paper presents a calculation method of loads induced by earthquake events on fuel assemblies, storage racks and civil structures of a water reactor spent fuel storage pool. Comparison between these loads, for different support designs, clearly shows that it is better to soften the links between racks and pool. Free translation is better than free rotation because no vertical load is induced by horizontal acceleration and horizontal loads on fuel assemblies, storage racks and pool are appreciably reduced. The aseismic bearing device developped by Framatome is the application of this principle. Its experimental qualification gives sufficient proves for safety purpose.

REFERENCES

/1/ FRITZ, R.J., "The effects of Liquids on the Dynamic Motions of Immersed Solids", Journal of Engineering for Industry, Translation of the ASME, Vol. 94, Feb. 1972, pp. 167-173

/2/ CEA Castem Computer Program
TIRDIR - Note EMT/SMTS/VIBR/80/33

Forces in kN Displacements in mm	Design 1	Design 2	Design 3
F1 - Reaction force at top	18.5	0	0
F2 - Reaction force at bottom	12.9	8.3	0.1
Fr - Hydrodynamic force on pool induced by racks	13.9	12.7	10.2
Fp - Hydrodynamic force on pool	16.5	16.2	13.2
Fa - Hydrodynamic force on cell	21.0	21.5	16.3
Fc - Impact force in one element	12.7	12.4	9.2
Fct- Total impact force on cell	25.6	27.5	17.7
FY - Vertical reaction force	-	40.5	
UX - Maximal horizontal displacement of cell	3	63	28

Table 1 : Maximal values of main results

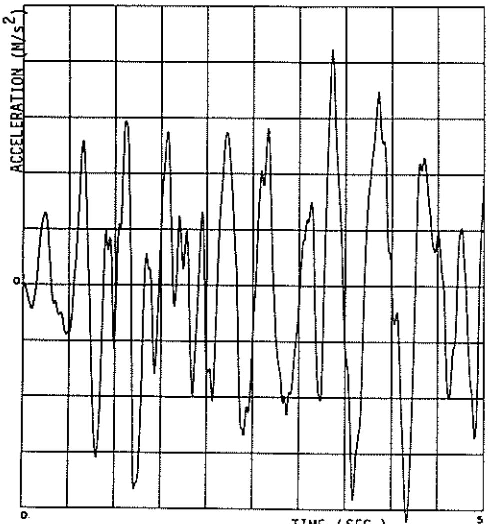

Fig. 5 : Seismic excitation

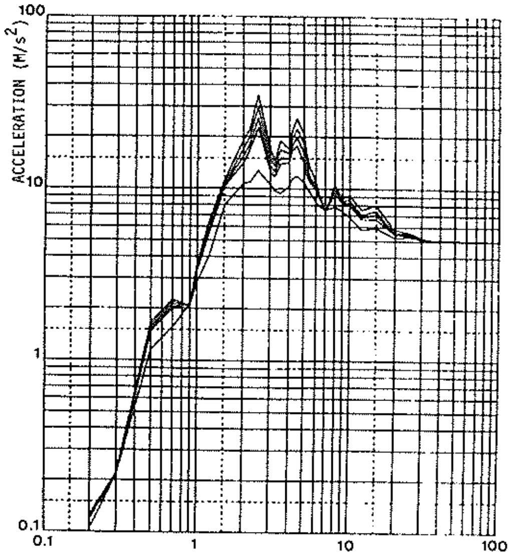

Fig. 6 : Response Spectrum

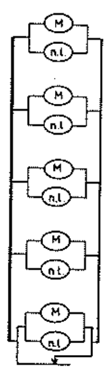

Fig. 1

Fig. 2

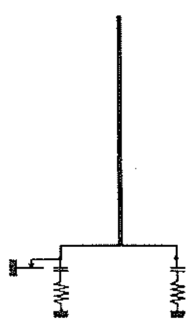

Fig. 3

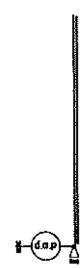

Fig. 4

LEGEND

M	Hydrodynamic Mass Matrix
n.l	Nonlinear element
dap	Aseismic bearing devices
	Friction element
	Gap element

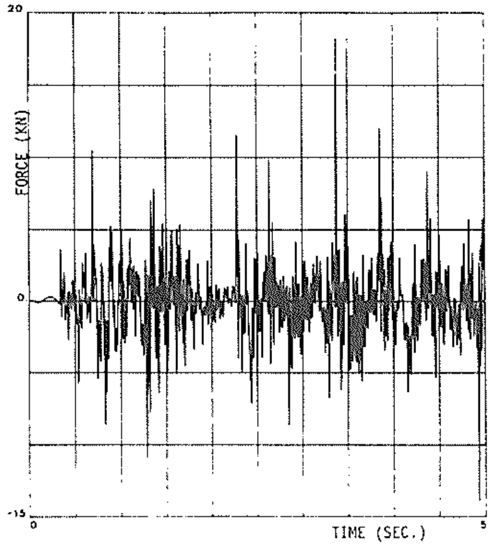

Fig. 7 : Design 1 - Reaction force at top

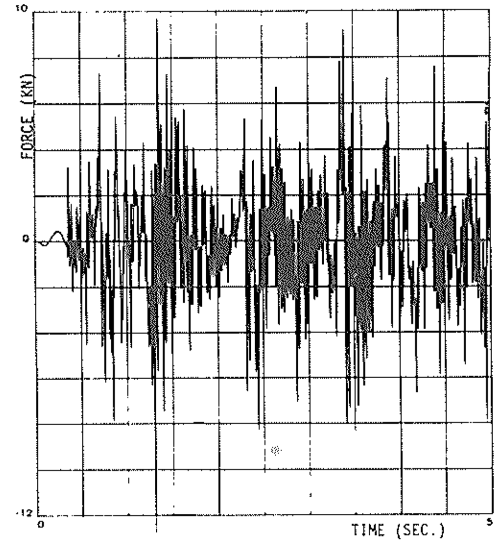

Fig. 8 : Design 1 - Reaction force at bottom

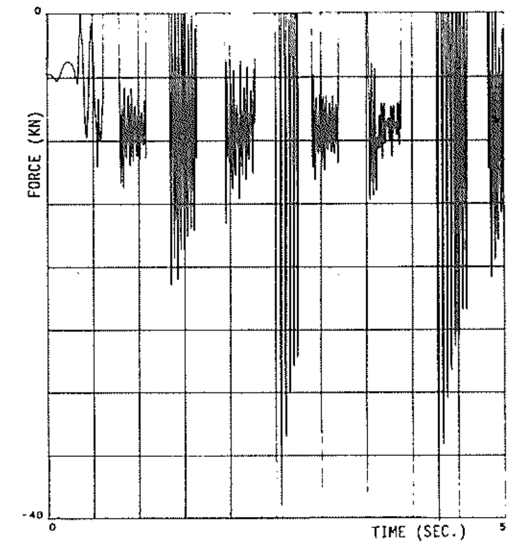

Fig. 9 : Design 2 - Vertical reaction force

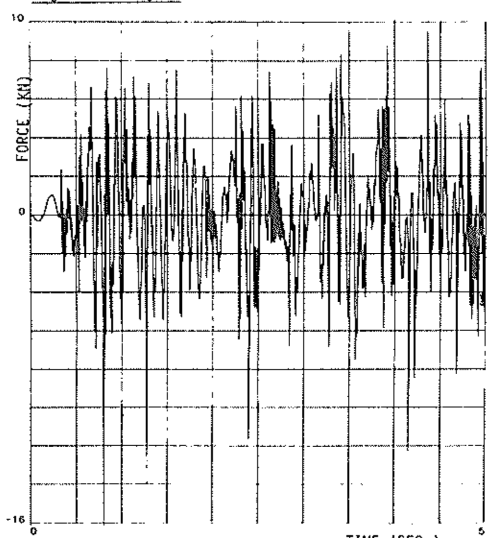

Fig. 10 : Design 1 - Hydrodynamic force on pool

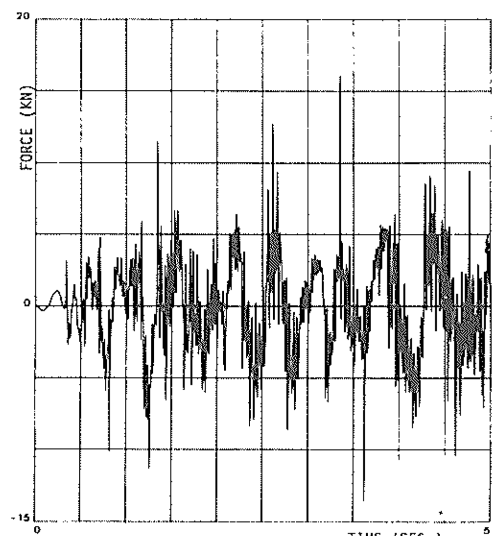

Fig. 11 : Design 2 - Hydrodynamic force on pool

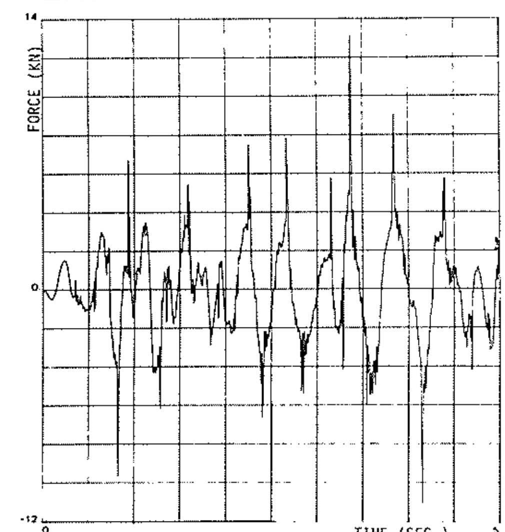

Fig. 12 : Design 3 - Hydrodynamic force on pool

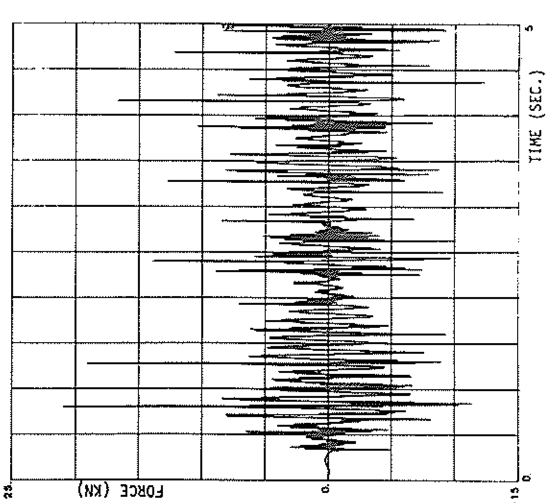

Fig. 13 : Design 1 Hydrodynamic force on cell

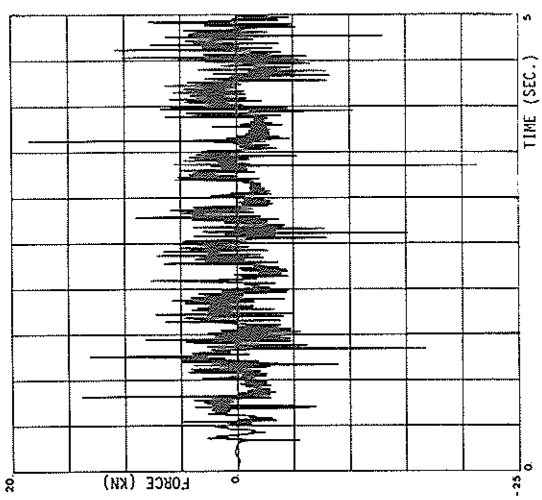

Fig. 14 : Design 2 Hydrodynamic force on cell

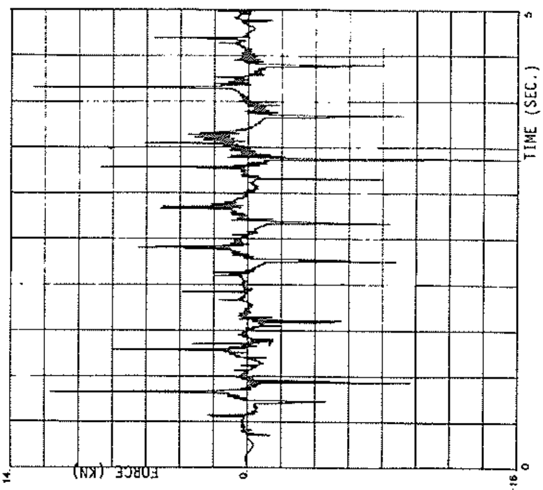

Fig. 15 : Design 3 - Hydrodynamic force on cell

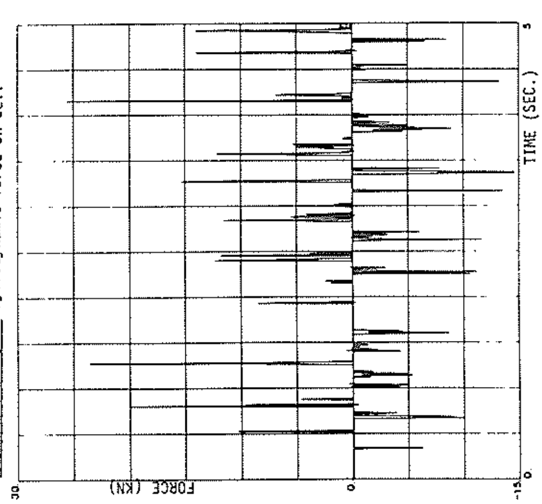

Fig. 16 : Design 1 - Total impact force on cell

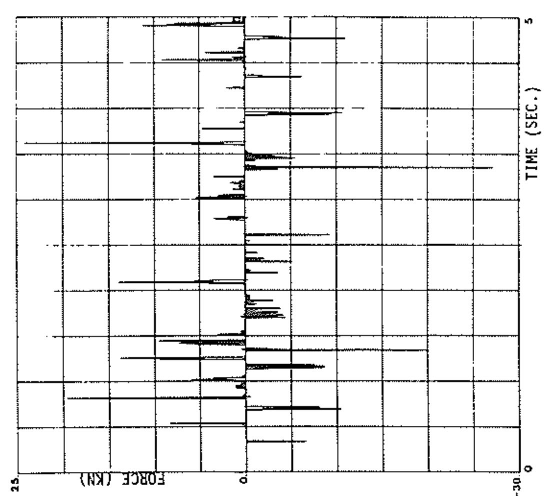

Fig. 17 : Design 2 - Total impact force on cell

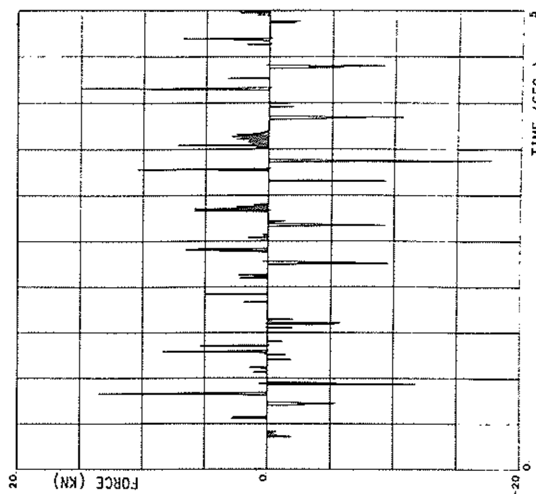

Fig. 18 : Design 3 - Total impact force on cell